AE geomagnetic index predictability for high speed solar wind streams: A wavelet decomposition technique*

Fernando L. Guarnieri[1], Bruce T. Tsurutani[2] Rajkumar Hajra[3], Ezequiel Echer[3] , Walter D. Gonzalez[3], and Anthony J. Mannucci[2]

[1] Vale, São José dos Campos, SP, Brasil

[2] Jet Propulsion Laboratory – JPL/NASA – Pasadena, CA, USA

[3] Instituto Nacional de Pesquisas Espaciais, São José dos Campos, SP, Brasil

F.L. Guarnieri, presented at IAGA, Perugia Italy, July 2007

Abstract

High speed solar wind streams cause geomagnetic activity at Earth. In this study we have applied a wavelet interactive filtering and reconstruction technique on the solar wind magnetic field components and AE index series to allowed us to investigate the relationship between the two. The IMF Bz component was found as the most significant solar wind parameter responsible by the control of the AE activity. Assuming magnetic reconnection associated to southward directed Bz is the main mechanism transferring energy into the magnetosphere, we adjust parameters to forecast the AE index. The adjusted routine is able to forecast AE, based only on the Bz measured at the L1 Lagrangian point. This gives a prediction ~30-70 minutes in advance of the actual geomagnetic activity. The correlation coefficient between the observed AE data and the forecasted series reached values higher than 0.90. In some cases the forecast reproduced particularities observed in the signal very well.

The high correlation values observed and the high efficacy of the forecasting can be taken as a confirmation that reconnection is the main physical mechanism responsible for the energy transfer during HILDCAAs. The study also shows that the IMF Bz component low frequencies are most important for AE prediction.

.

CORRELATED ACTIVITY

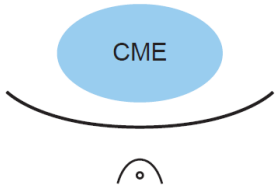

Long Period Alfvén Wave

NON CORRELATED ACTIVITY

Medium Period Alfvén Wave

Different Parts of Magnetosphere
Have Different Stimuli

Long Period Alfvén Wave

Internal Chaos

Alfvén Wave Misses Magnetosphere

High Speed Solar Wind Streams

- High velocity flows emanating from coronal holes.
- These streams contain highly fluctuating magnetic fields, nonlinear Alfvén waves.
- The southward component of the Alfven waves lead to magnetic reconnection at the dayside magnetopause and intense auroral zone geomagnetic activity called HILDCAAs.

HILDCAA events

High Intensity, Long Duration, Continuous AE Activity (Tsurutani and Gonzalez, 1987)

HILDCAA Criteria:

- The AE peak must reach, at least, **1000 nT**;
- The event must last for, at least, **two days**;
- The AE values cannot decrease to **less than 200 nT for more than 2 hours** at a time;
- The event must occur **outside the main phase of a geomagnetic storm**.

These events are **NOT simply a series of substorms**. Although substorms are occurring during HILDCAAs more is happening as well. (Tsurutani et al., 2004; Guarnieri et al., 2004; Guarnieri, 2005; Guarnieri, 2006)

HILDCAA effects

- Weak to moderate geomagnetic Dst or SYM-H activity.

- Very intense auroral electrojet activity (AE index);

- HILDCAA auroras are mild, but widely spatially distributed (even on the dayside) and long lasting. Guarnieri (2007) had shown (using POLAR images) that the integrated emissions during these auroras can be even higher than those observed during some very intense geomagnetic storms;

- During these prolonged intervals of HILDCAAs, **increased fluxes of relativistic electrons are observed, which can have significant impact over satellite systems** (Hajra et al., 2013; 2014a,b).

Events List

Year	Event	Start	End	Lenght (min)
1998	1	April 24, 18:03	April 27, 06:05	3603
	2	July 22, 21:09	July 25, 12:25	3797
1999	1	April 29, 11:20	July 03, 11:16	5757
	2	August 17, 22:528	August 20, 12:00	3669
	3	August 31, 15:32	September 02, 20:30	3179
	4	October 10, 20:00	October 14, 17:38	5619
	5	October 23, 13:21	October 25, 20:57	3337
	6	November 07, 17:00	November 10, 04:47	3588
	7	December 03, 10:00	December 06, 00:15	3736
2000	1	January 27, 18:10	January 31, 03:15	4866
	2	February 05, 16:01	February 08, 05:33	3693
	3	February 24, 00:03	Februray 27, 22:10	5648
	4	May 24, 10:00	May 26, 18:07	3368
2001	1	May 11, 14:04	May 26, 14:10	4128

Table 1 – HILDCAA events used in this analysis. All the events above follow strictly the HILDCAA criteria. These events were previously identified by Guarnieri (2005).

HILDCAA events

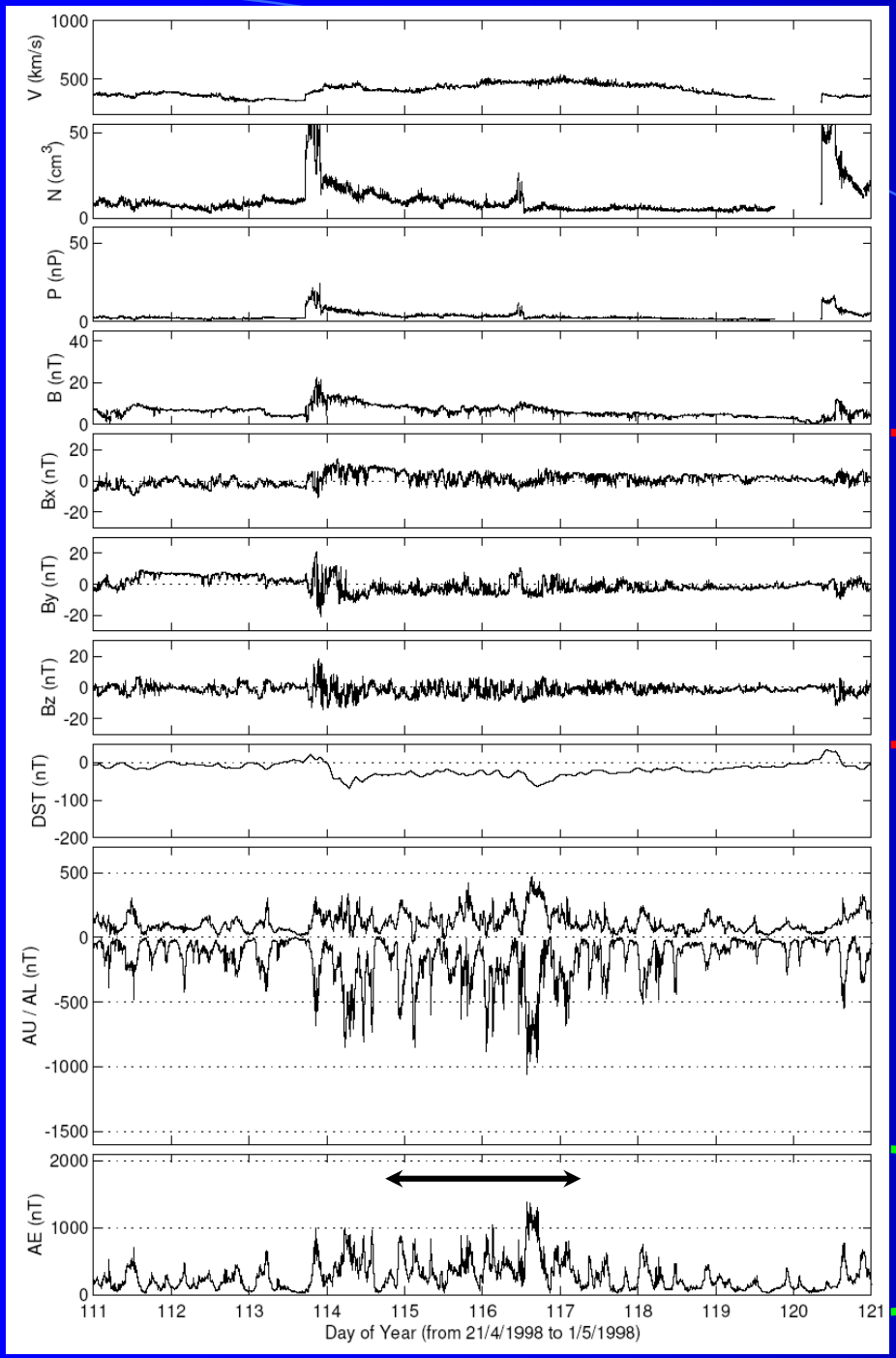

Magnetic field component plots indicating the presence of Alfvénic fluctuations in the solar wind.

The black arrow indicates the HILDCAA event duration.

HILDCAA events

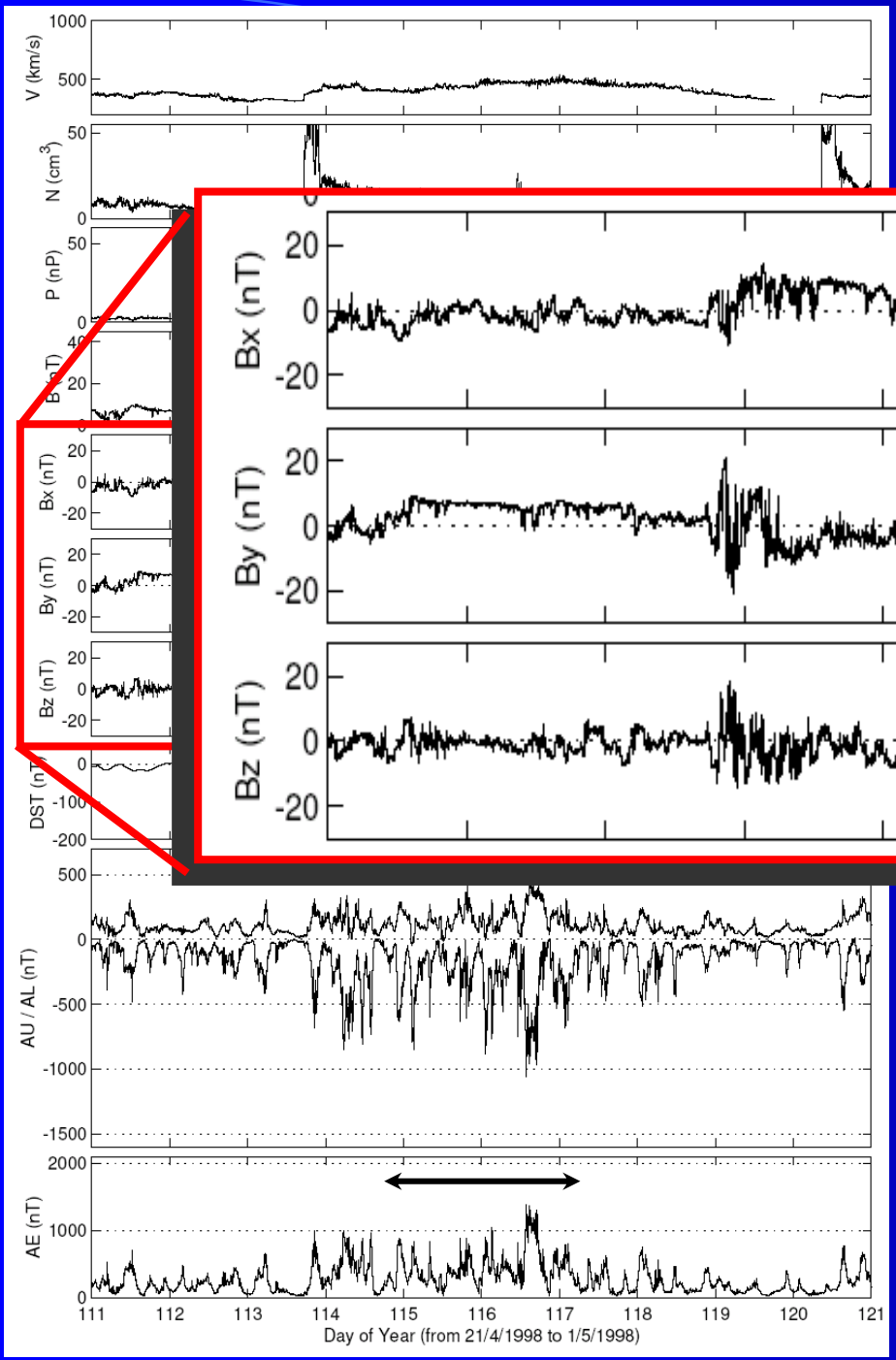

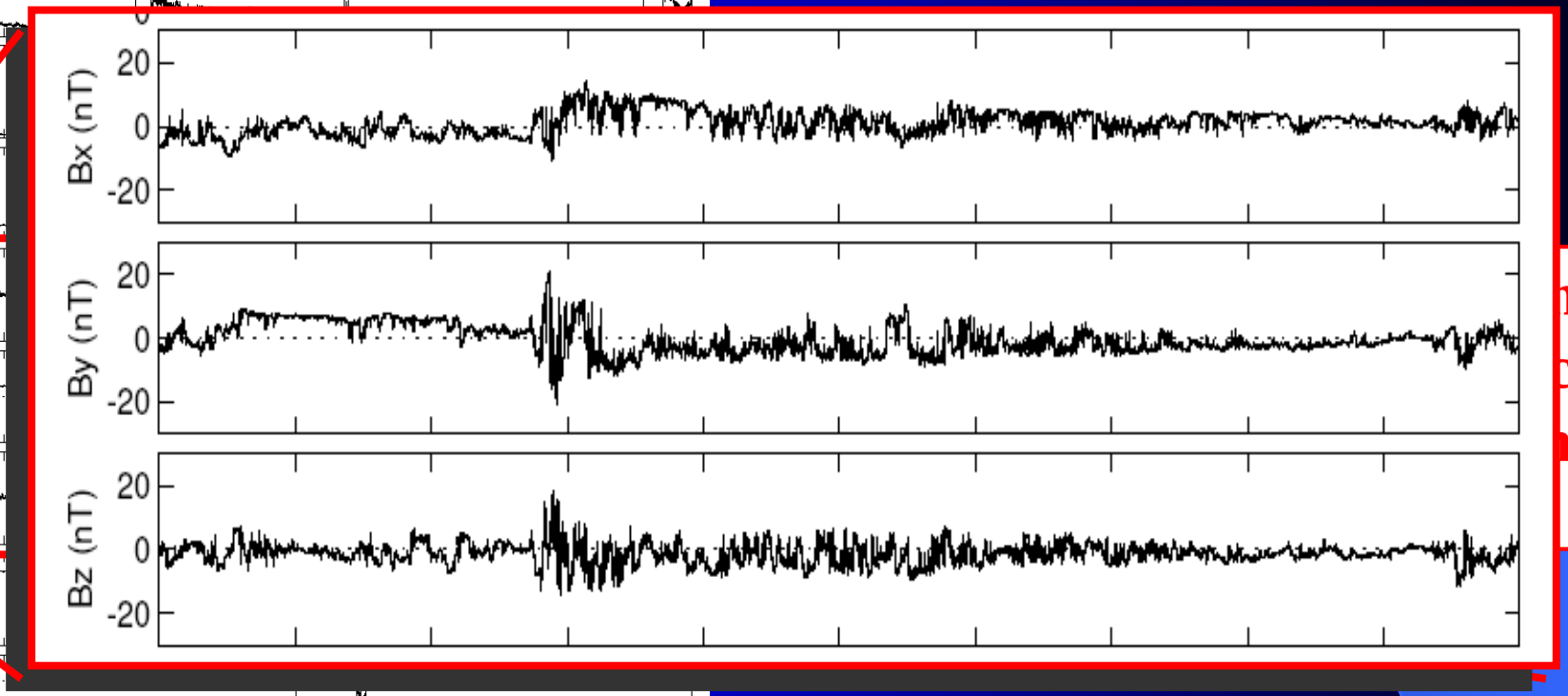

Estimative Techniques

- CMEs, Magnetic Clouds
  - Burton (1975) – Dst index estimative
  - Chen (1997) – Dst index estimative
  - Ahn et al. (1981) – AE index estimative
- High Speed Streams/Alfvén waves
- Since the first HILDCAA observations by Tsurutani and Gonzalez, a very poor correlation has been noted between interplanetary parameters and the AE index.
- In this work we show a technique that estimates the AE index intensity based only on interplanetary data.

Methodology

Data sets:

-Interplanetary magnetic field (IMF)
-Solar wind parameters

} ACE spacecraft (MAG and SWEPAM instruments) 1-minute time resolution - Level 2

AE index } *Word Data Center for Geomagnetism* (Kyoto) 1-minute time resolution

Techniques:

- Meyer wavelet decomposition technique: employed to analyze Bz and AE data series for 14 HILDCAA events occurred from 1998 to 2001 (events previously identified by Guarnieri, 2005).

- Cross-Correlation technique adapted to analyzed different bands from the decomposition results.

- With the decomposition and reconstruction results in each level, for both the AE and Bz, a routine was developed to adjust the weights of an equation to estimate the AE index based only on Bz, aiming the highest possible correlation coefficient.

Periods and ranges for the Meyer wavelet decomposition technique

Level	n	Period	Range (minutes)
D1	1	2	0-2
D2	2	4	2-4
D3	3	8	4-8
D4	4	16	8-16
D5	5	32	16-32
D6	6	64	32-64
D7	7	128	64-128
D8	8	256	128-256
D9	9	512	256-512
D10	10	1024	512-1024
A10			>1024

Table 2 – Periods and ranges related to each level used in the wavelet decomposition technique. The bands are multiples of 2^n.

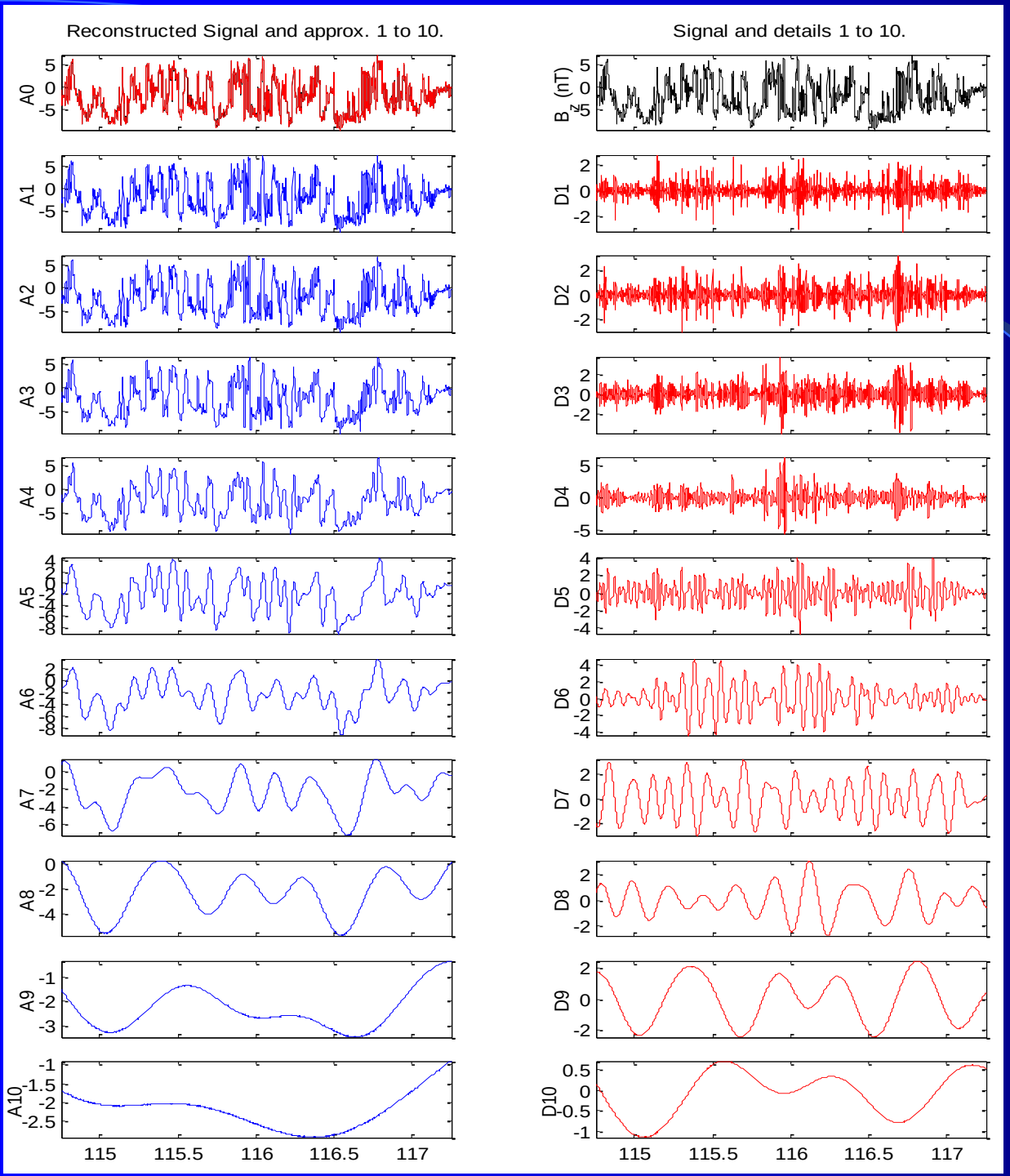

Figure 1 – Wavelets decomposition for the interplanetary magnetic field Bz component for the event 1_1998. On the right side are the decompositions, with the bands from D1 to D9. The "rest" of the process is stored in the level A10. The left side shows the approximations, which are the sum of the decompositions (from bottom to top)

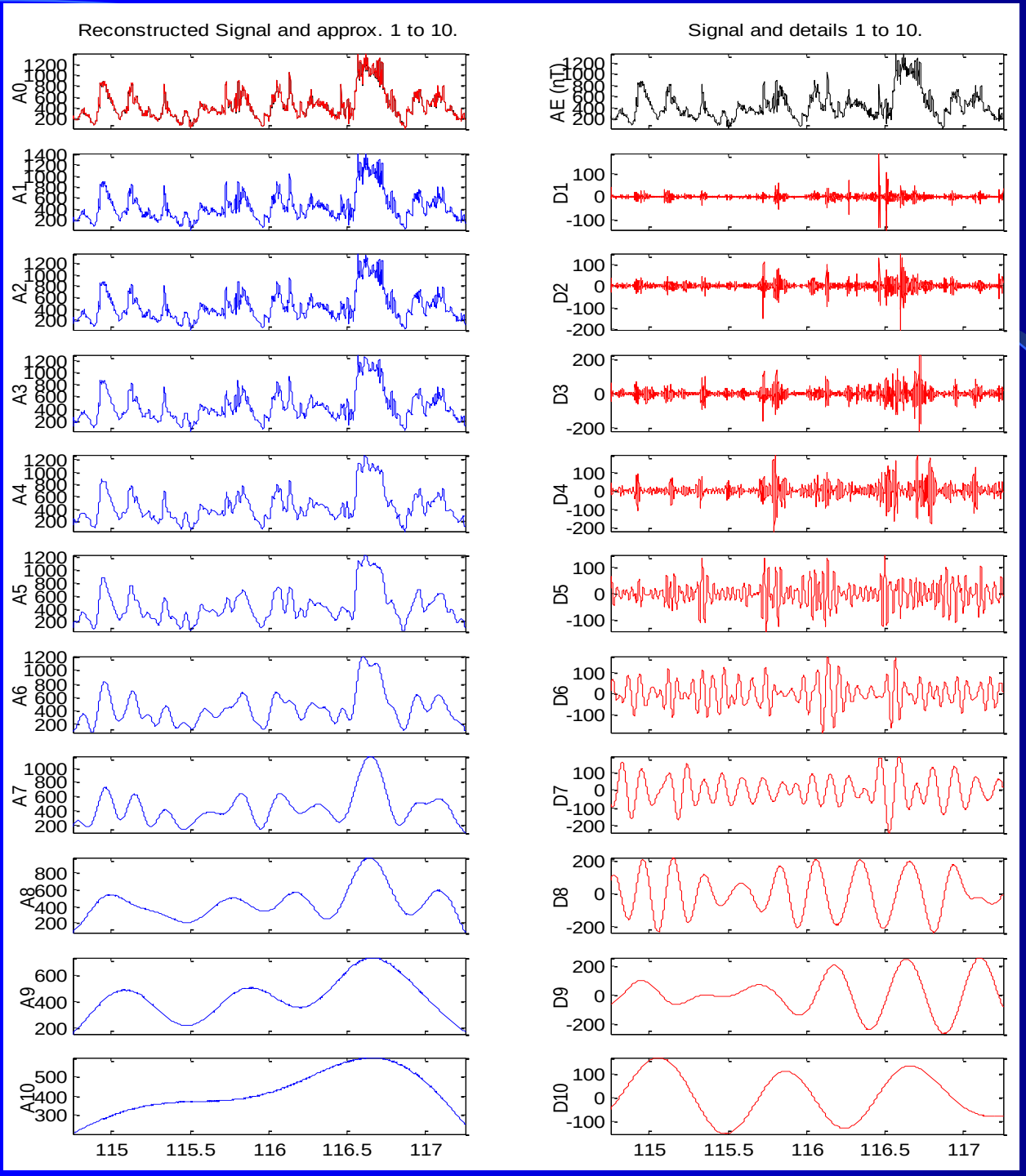

Figure 2 – Wavelet decomposition for the AE index. The bands are shown in the right side. The left side show the approximations. The approximations are equivalent to an adjustable low-pass filter.

AE/Bz Correspondence

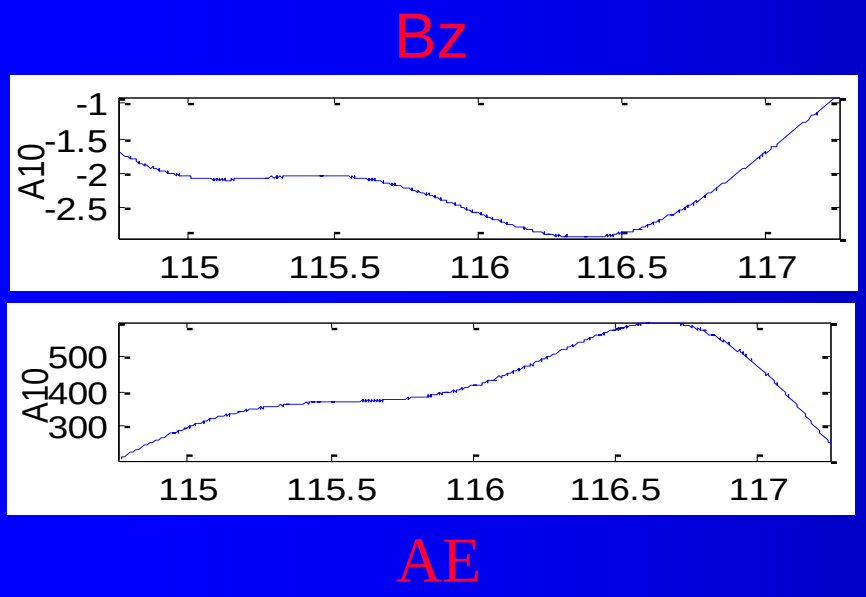

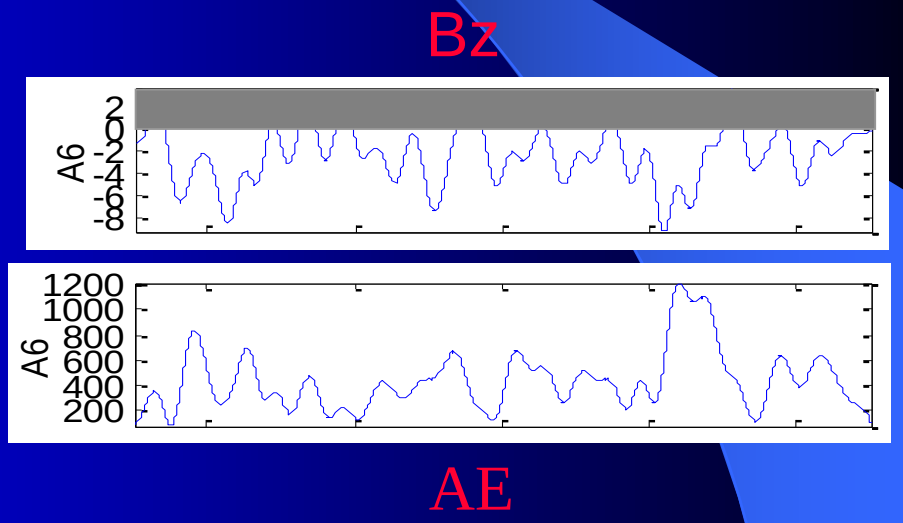

Figure 3 – Comparison between AE and Bz for the level A10 (left) and level A6 (right). A good correlation is observable although the existence of a lack due to the propagation time for the Bz from the ACE to the Earth plus the magnetospheric response time.

Preliminary Model

NBz = shifted Bz time series using solar wind velocity and considering a magnetospheric response time;
ANBz = approximation for the NBz;
ANAE = approximation for the AE time series;

If Bz < 0

$$\mathbf{ANAE_{(t)} = \alpha + \beta.ANBz_{(t)}}$$

If Bz > 0

$$\mathbf{ANAE_{(t)} = \alpha}$$

where $\alpha, \beta, \varepsilon,$ and γ are adjustable variables.

Simplified model

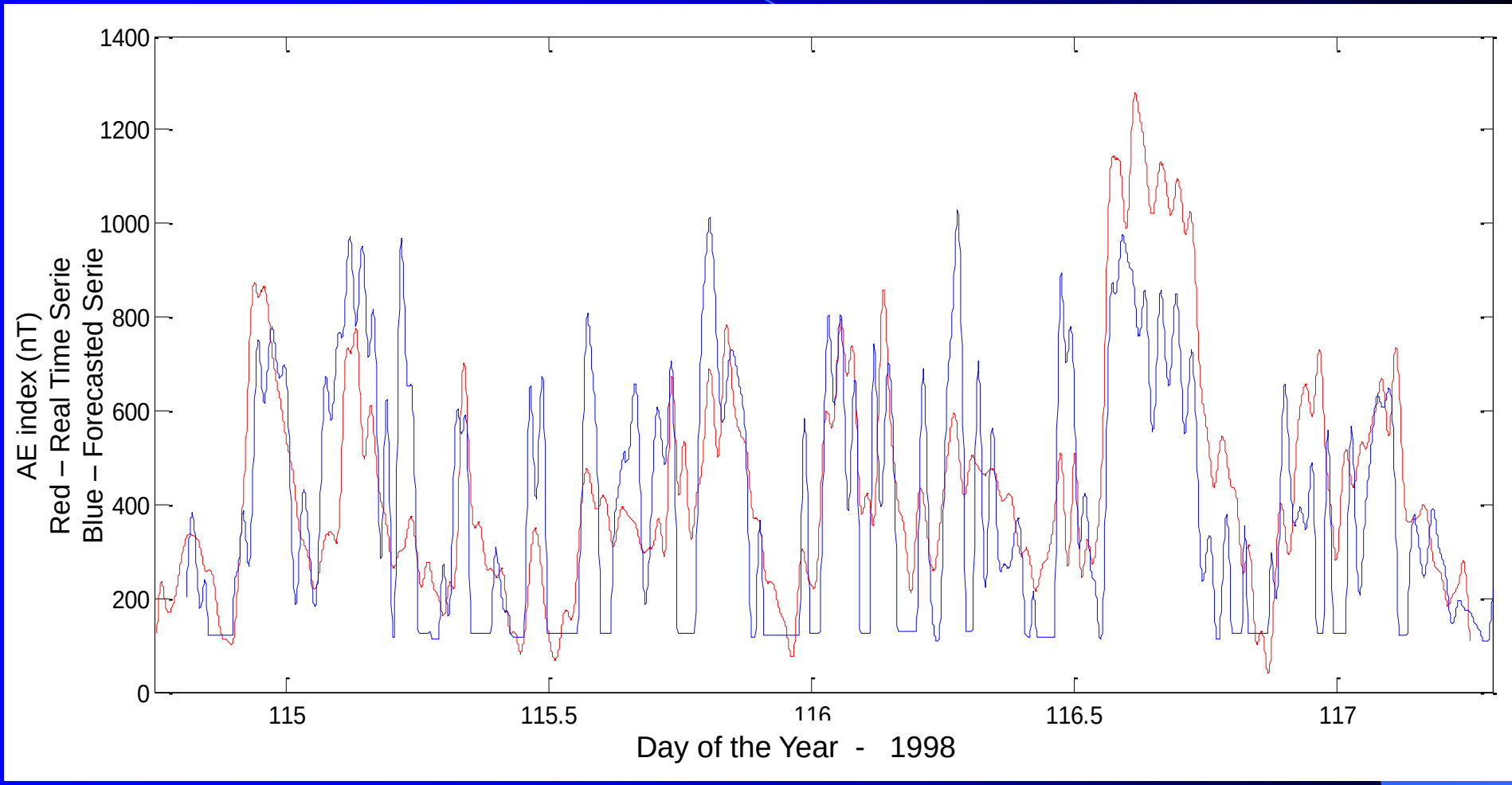

Figure 4 – Simplified model for the AE index forecasting based only on Bz. The red line represents the real values observed. The blue line represents the forecasted series.

Model

NBz = shifted Bz time series;
ANBz = approximation for the NBz;
ANAE = approximation for the AE time series;

If Bz < 0

$$ANAE_{(t)} = \alpha + \beta . ANBz_{(t)}$$

If Bz > 0

$$ANAE_{(t)} = ANAE_{(t-1)} - e^{(\gamma . |-ANBz|)}$$

where $\alpha, \beta,$ and γ are adjustable variables.

β =150
α=70 nT
γ=1

Final Model

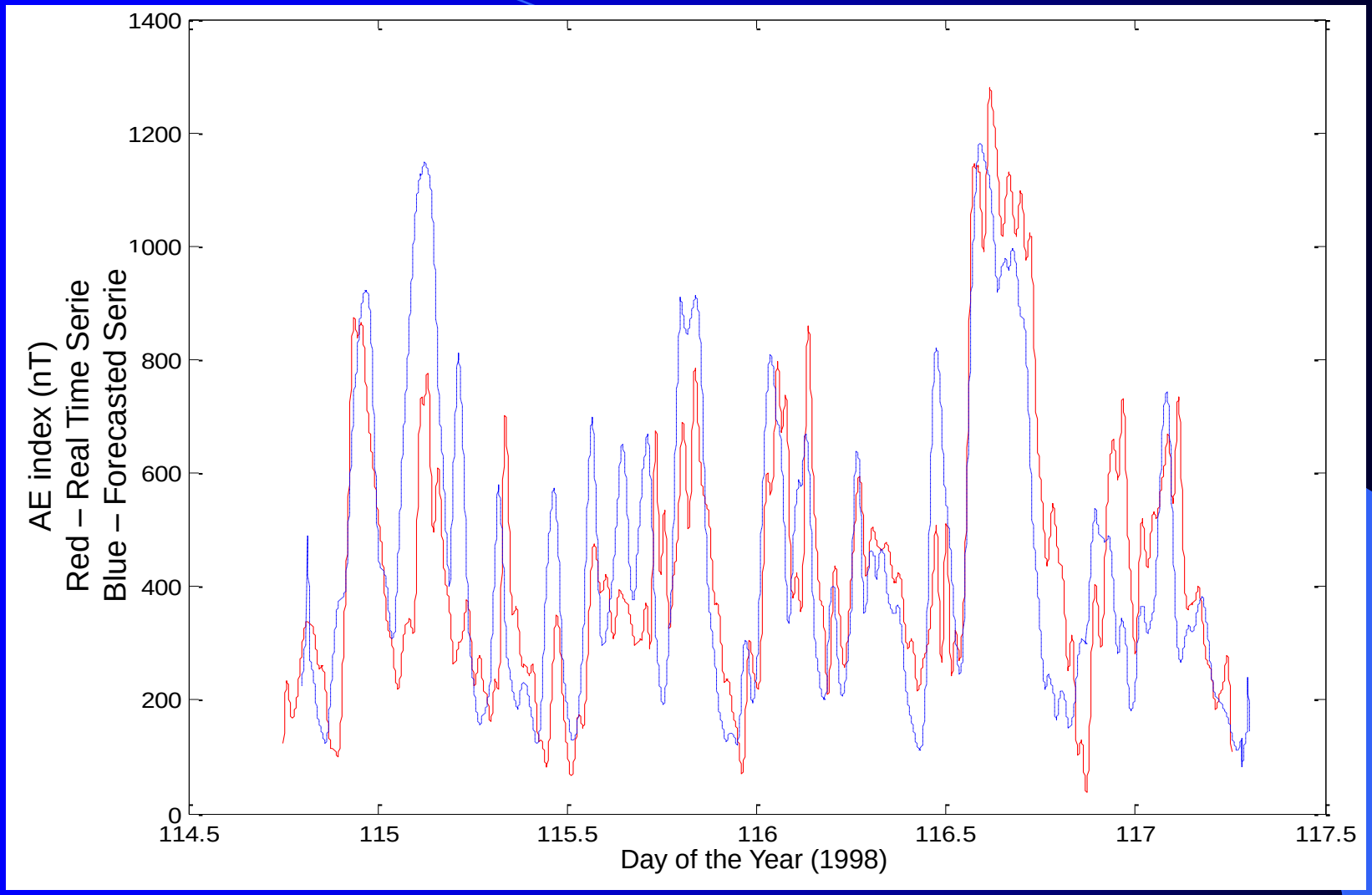

Figure 5 – Final model for AE forecasting. The red line represents the real data series observed. The blue line indicates the forecasted AE time series. The final model reproduces more accurately the valleys and significantly increased the correlation between the two series. For this specific case, the correlation coefficient was 0.948.

Event	A3	A4	A5	A6	A7	A8	A9
ev1_1998	0.943	0.947	0.948	0.944	0.926	0.928	0.977
ev2_1998	0.913	0.908	0.903	0.907	0.936	0.892	0.894
ev1_1999	0.920	0.920	0.926	0.924	0.931	0.920	0.946
ev2_1999	0.876	0.875	0.865	0.884	0.860	0.853	0.879
ev3_1999	0.958	0.962	0.964	0.965	0.982	0.990	0.995
ev4_1999	0.893	0.889	0.875	0.845	0.844	0.855	0.941
ev5_1999	0.918	0.922	0.915	0.904	0.912	0.901	0.943
ev6_1999	0.921	0.919	0.918	0.902	0.910	0.847	0.863
ev7_1999	0.892	0.887	0.880	0.863	0.857	0.873	0.867
ev1_2000	0.708	0.735	0.866	0.917	0.528	0.542	0.555
ev2_2000	0.856	0.859	0.872	0.891	0.900	0.878	0.890
ev3_2000	0.790	0.597	0.589	0.541	0.443	0.407	0.436
ev4_2000	0.936	0.937	0.936	0.867	0.878	0.906	0.956
ev1_2001	0.908	0.909	0.905	0.906	0.893	0.899	0.925
Average	0.888	0.876	0.883	0.876	0.843	0.835	0.862

Table 3 – Correlation coefficients for several filtering levels. The last line has the average value for the correlation coefficients of each column. Although this average does not have any physical meaning, it was used only as an indicative of the correlation performance.

Event	A3	A4	A5	A6	A7	A8	A9
ev1_1998	0.943	0.947	0.948	0.944	0.926	0.928	0.977
ev2_1998	0.913	0.908	0.903	0.907	0.936	0.892	0.894
ev1_1999	0.920	0.920	0.926	0.924	0.931	0.920	0.946
ev2_1999	0.876	0.875	0.865	0.884	0.860	0.853	0.879
ev3_1999	0.958	0.962	0.964	0.965	0.982	0.990	0.995
ev4_1999	0.893	0.889	0.875	0.845	0.844	0.855	0.941
ev5_1999	0.918	0.922	0.915	0.904	0.912	0.901	0.943
ev6_1999	0.921	0.919	0.918	0.902	0.910	0.847	0.863
ev7_1999	0.892	0.887	0.880	0.863	0.857	0.873	0.867
ev1_2000	0.708	0.735	0.866	0.917	0.528	0.542	0.555
ev2_2000	0.856	0.859	0.872	0.891	0.900	0.878	0.890
ev3_2000	0.790	0.597	0.589	0.541	0.443	0.407	0.436
ev4_2000	0.936	0.937	0.936	0.867	0.878	0.906	0.956
ev1_2001	0.908	0.909	0.905	0.906	0.893	0.899	0.925
Average	0.888	0.876	0.883	0.876	0.843	0.835	0.862

Table 3 – Correlation coefficients for several filtering levels. The last line has the average value for the correlation coefficients of each column. Although this average does not have any physical meaning, it was used only as an indicative of the correlation performance.

Conclusions

The Bz component was found as the most significant solar wind parameter responsible by the control of the AE activity.

The adjusted routine is able to forecast AE, based only on the Bz measured at the L1 Lagrangian point. This will give us a prediction ~ 40 minutes in advance of the actual auroral activity.

Use of some of the lowest orders (A9) appears to work well, in general. To go down to the A5 level improves the predictability of AE, but only slightly.

Conclusions

- The highest frequency terms only add noise to the system and leads to decorrelation.
- Can VTEC be similarly correlated with AE wavelet decomposition?
- Can the technique be improved or is this a physical limitation of the data?
-

CORRELATED ACTIVITY

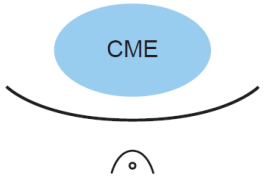

Long Period Alfvén Wave

NON CORRELATED ACTIVITY

Medium Period Alfvén Wave

Different Parts of Magnetosphere
Have Different Stimuli

Long Period Alfvén Wave

Internal Chaos

Alfvén Wave Misses Magnetosphere

Acknowledgments

- ACE data center for the interplanetary data;
- Word Data Center for Geomagnetism – Kyoto for the geomagnetic indices.
- Portions of this work were done at the Jet Propulsion Laboratory, California Institute of Technology under contract with NASA

Thank you for your attention !!!